from *SIAM News*, Volume 35, Number 2

Hydrodynamic Instability in Two and Three Dimensions

By James Case

Caltech applied mathematician Thomas Hou, who has put his research in multiscale problems to work for SIAM (see sidebar), also lists turbulence in fluid flow among his research interests. In recent work, he and colleagues succeeded in extending two-dimensional analyses of Kelvin–Helmholtz instability to three dimensions.

Hou presented these results at the first SIAM–EMS Conference, "Applied Mathematics in our Changing World," held at ZIB (the Konrad-Zuse-Zentrum für Informationstechnik Berlin), September 2–6. James Case describes the new results here, concluding that Hou and his colleagues have brought "the ever distant goal" of understanding turbulence and hydrodynamic instability at least a few steps closer.

One of the most telling experiments in the entire history of fluid dynamics was performed by Osborne Reynolds in 1883. While studying the flow of water through a horizontal glass tube, he injected a small quantity of colored water into the middle of the stream, near the intake, at the same pressure and temperature as the clear feed-stock. At low velocities, Reynolds found the flow to be smooth, or laminar, with each fluid particle traveling in a straight line parallel to the axis of the tube.

As the speed was gradually increased, however, the colored streak would suddenly begin to mix—some distance downstream—with the surrounding water, filling the entire breadth of the tube with a cloudy mass of unevenly colored liquid. When backlit by an intermittent spark (in lieu of stop-action photography), the cloud resolved itself into a mass of more or less distinct curls and eddies. The sudden transition from smooth, laminar flow to turbulence as the fluid velocity is gradually increased remains one of the least adequately explained phenomena in all of classical physics.

Smooth rectilinear flow through a tube of circular cross section remains a valid solution of the Navier–Stokes equations (and relevant boundary conditions) at all flow speeds. It is not, however, a "stable" solution—at high speeds, unavoidable small shocks to the experimental apparatus invariably cause such flows to "morph" quite suddenly into more complicated ones. The relevant boundary value problem is known [1] to be ill-posed in the Hadamard sense. That is presumably the reason for the failure of recent attempts to reproduce Rey-nolds's original results in his original basement laboratory at the University of Manchester (UK)—even late at night, vibrations from traffic in the surrounding streets cause the onset of turbulence to occur at lower flow speeds than of old.

Classic Kelvin–Helmholtz Instability

A classic example of hydrodynamic instability occurs when two fluids are separated by a free surface S across which the tangential (but not the normal) component of the fluid velocity exhibits a jump discontinuity. Such surfaces occur naturally on the downstream side of an obstacle—such as the wing of an airplane—where they separate the particles of fluid that passed over the obstacle from those that went under it. At very slow speeds, such surfaces S can hold their shapes indefinitely, as they are convected along with the fluid. But at higher speeds they can—suddenly and without apparent warning—be crumpled like a sheet of typing paper into a thoroughly irregular shape. Such behavior, known as Kelvin–Helmholtz instability, ranks among the most extensively studied forms of hydrodynamic instability.

For purposes of analysis, S is ordinarily assumed to be an orientable surface on either side of which the fluid velocity, density, and stress—along with their low-order space derivatives—can be extended by continuity to S. If $\mathbf{n}$ denotes the (upward) unit normal vector to S, while $\mathbf{v}^+$ and $\mathbf{v}^-$ denote the fluid velocities immediately above and below S, then $\Omega = (\mathbf{v}^+ - \mathbf{v}^-) \times \mathbf{n}$ defines a vector field tangent to S; the magnitude ω of Ω is known as the "vortex strength" of the flow near S. Any curve Γ on S that is everywhere tangent to the Ω field is known as a "vortex line" on S. (Ω is not to be confused with the mean flow velocity $\mathbf{v}_{avg} = (\mathbf{v}^+ + \mathbf{v}^-)/2$, which is also of interest in the study of vortex sheets.)

Kelvin–Helmholtz instability is most frequently studied in the context of two-dimensional flow, where methods of complex variables can be exploited. In 1979, Moore [6] allowed $r(\alpha,t) = x(\alpha,t) + i\,y(\alpha,t)$ to denote the position of a particular particle $\alpha \in C = S \cap \pi$ at times $t \geq 0$, where π is a plane left invariant by the 2D flow. Thus, α serves as a parameter along the curve C that might (but need not) coincide with the arclength s measured along C from a distinguished particle α_0 at which $\alpha = 0$. If ρ^+ and ρ^-, the fluid densities immediately above and below S, are equal while the velocity of the interface is chosen to be the average of $\mathbf{v}^+$ and $\mathbf{v}^-$, $r(\alpha,t)$ can be shown to satisfy the Birkhoff–Rott equation [1]:

$$\frac{\partial \bar{r}(\alpha,t)}{\partial t} = \frac{1}{2\pi i}\,\mathrm{CPV}\int_{-\infty}^{\infty} \frac{\gamma(\alpha',t)}{r(\alpha,t)-r(\alpha',t)}\,d\alpha', \tag{1}$$

in which CPV stands for Cauchy principal value and $\gamma(\alpha,t)$ is related to the vorticity field strength $\omega = \omega(\alpha,t) = \gamma(\alpha,t)/((\partial x/\partial\alpha)^2 + (\partial y/\partial\alpha)^2)^{1/2}$. If C coincides at time $t = 0$ with a periodically perturbed segment of the horizontal axis, so that $x(\alpha,0) = \alpha$ and $y(\alpha,0) = f(\alpha)$, where f is a periodic function, while the vortex sheet strength $\gamma(\alpha,0) \equiv 1$, then $r(\alpha,t)$ also satisfies a periodic version of (1). In it, the kernel $1/(r(\alpha,t) - r(\alpha',t))$ is replaced by the cotangent kernel

$$\cot\left(\frac{1}{2}\left(r(\alpha,t)-r(\alpha',t)\right)\right), \quad (2)$$

and the integral runs from 0 to L, the period of f. Numerical and other analysis of this periodic version of (1) by Moore [6] and others suggests that S develops a weak singularity after the passage of a fixed amount of time.

The focus of Moore's work, and the flurry of activity it spawned, is on the flow transition that occurs at the end of this fixed (and approximately computable) amount of time. Reynolds's experiment revealed a critical distance beyond which the flow ceased to follow simple rectilinear flow lines. Moore, and those who followed his lead, found that as vortex sheets evolve, there comes a critical instant after which a previously regular sheet S may become highly irregular, at least in the vicinity of certain isolated points.

Although the early, precritical, and critical sheets S exhibited in Figure 2 (a, b, and c, respectively) don't look all that different from one another, the corresponding plots of their absolute curvatures (shown in Figure 1a, b, and c) differ more perceptibly. In particular, the critical curve of Figure 1c exhibits a cusp (sharp peak) at its intersection with the line $x = 0$, which seems mysteriously to cause the irregular flows observed subsequently nearby.

Solutions of the periodic version of (1) for which $f(\alpha) = \varepsilon \sin \alpha$ can be expanded in a (complex, infinite) Fourier series with time-varying coefficients,

$$r(\alpha,t) = \alpha + \textstyle\sum_m A_m(t)\exp(im\alpha), \quad (3)$$

where m runs through the (positive and negative) integers and $A_m = -A_{-m}$ in every case. Substitution of (3) into the periodic version of (1) yields an infinite system of first-order ordinary differential equations for the quantities $A_m(t)$. Expansion in increasing powers of ε gives

$$A_m(t) = \varepsilon^{|m|}A_{m0}(t) + \varepsilon^{|m+2|}A_{m2}(t) + \varepsilon^{|m+4|}A_{m4}(t) + \ldots, \quad (4)$$

along with a "leading-order" subsystem involving only the $A_{m0}(t)$ that is simple enough to study in detail. At a critical time $\tau = \tau(\varepsilon)$ given to first order by

$$1 + \tau/2 + \ln(\tau) = \ln(4/\varepsilon), \quad (5)$$

the coefficients A_{m0} begin to decay as $m^{-5/2}$—rather than exponentially—suggesting that r is no longer analytic in α. To confirm that the asymptotic expressions obtained for small values of ε are tol-erably accurate, Damms (unpublished, 1978) integrated numerically a truncated version of the ODEs satisfied by the quantities $A_m(t)$.

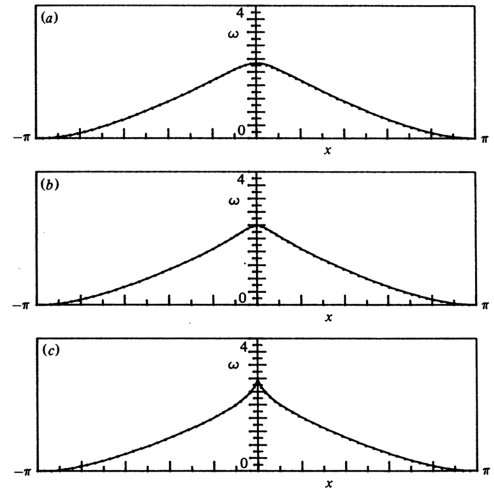

Figure 1. *Plots of the vortex sheet strength ω(x,t) long before (a), just before (b), and at (c) the singularity time t = τ. A cusp appears at the roll-up point x = 0 when t = τ.*

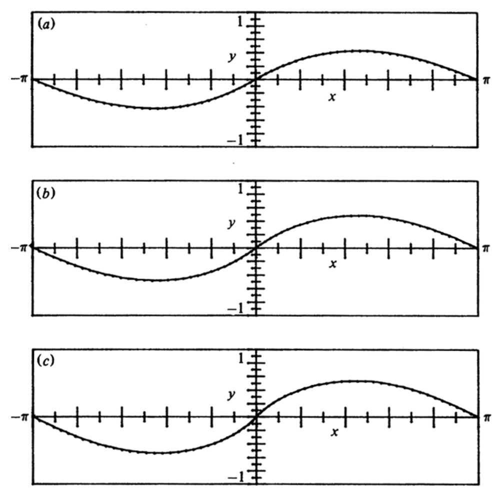

Figure 2. *Plots of the interface r(x,t) at comparable times. Notice that the interface is still only slightly deformed at t = τ.*

Others [5] soon solved the periodic version of (1) with initial data: $\gamma(\alpha,0) = 1 + \varepsilon \cos \alpha$; $r(\alpha,0) = \alpha$, in part by observing that the coefficients $R_n(\alpha)$ in the expansion

$$r(\alpha,t) = \alpha + \textstyle\sum_n R_n(\alpha)t^n, \quad (6)$$

are finite Fourier series of the form $\sum_m R_{nm} \sin m\alpha$. Moreover, using symbolic computation, they were able to generate $R_1(\alpha), \ldots, R_7(\alpha)$ in closed form, and to confirm that the results compare favorably with numerically calculated values. Such findings further confirm Moore's conclusion that the sheet S develops a singularity at a time $t = \tau$ consistent with (5).

It would doubtless be more interesting to know how the roll-up of S continues after the onset of singularity, but experiment shows that the results obtained from the approximate solution of (1) are not to be trusted after $t = \tau$. Thus, at least for the moment, the results obtained from this line of inquiry pertain only to the very onset of turbulence. Other physical regularizations, such as viscosity or surface tension, are clearly needed for study of the solution beyond the singularity time.

Extension to the Complex Plane

In a somewhat more general approach [2], $r(\alpha,t) = \alpha + \xi(\alpha,t)$ and $\gamma(\alpha,t) = \alpha + \eta(\alpha,t)$, so that ξ and η become the 2π-periodic parts of r and γ, respectively. Then α is allowed to assume complex as well as real values, and an operator * is defined by $f^*(\alpha,t) = \overline{f(\bar{\alpha},t)}$, so that $f^*(\alpha,t)$ is an analytic function of α if and only if f is one. Moreover, (i) if ξ and ξ* are known in the upper half of the α-plane, then ξ is known in the entire α-plane; (ii) if ξ is *typically real*, so that ξ is real whenever α is real, then $\xi^* = \xi$ for all α; and (iii) when α is real, then $\xi^*(\alpha,t) = \overline{\xi(\overline{\alpha},t)}$. Using contour deformation and complex analysis, the periodic version of (1) can be rewritten in the following two ways:

$$\partial\xi^*/\partial t = (\eta_\alpha - \xi_\alpha)/2(1 + \xi_\alpha) + J(\alpha,t)$$

$$\partial\xi/\partial t = (\xi^*_\alpha - \eta_\alpha/2(1 + \xi^*_\alpha) + K(\alpha,t). \tag{7}$$

The first terms on the right-hand sides represent the leading-order near-field contributions, i.e., when α' is close to α in (1), and J and K are certain Cauchy principal value integrals representing far-field contributions that can on occasion be ignored.

The solutions ξ and ξ^* of the resulting pair of partial differential equations can be expected to exhibit singularities at points $\alpha \in \mathbb{C}$ at which either or both of the quantities $1 + \xi_\alpha$ and $1 + \xi^*_\alpha$ vanish. Returning to the initial conditions $\xi(\alpha,0) = 0$ and $\eta(\alpha,0) = \varepsilon \sin(\alpha)$ considered in [4] above, and assuming $t << 1$, ξ and ξ^* can be shown to have such singularities at $\alpha = i\cdot\ln(2/\varepsilon t)$, which propagate from $\alpha = \infty$ toward the real line as t increases.

Furthermore, properties (i)–(iii) of the * operator imply that the analytic continuation of ξ into the lower half of the α-plane has a singularity at $\overline{\alpha}$ whenever ξ^* has one at α in the upper half-plane. Moreover, the order of these singularities remains constant and equal to 3/2 as they propagate about $\mathbb{C}$, and the vortex sheet S: $r(\alpha,t)$ develops a singularity when these moving complex singularities strike the real line. Indeed, the same qualitative behavior can be demonstrated for a fairly extensive class of initial conditions $\xi(\alpha,0)$ and $\eta(\alpha,0)$. Finally, on the assumption that the physical singularity occurs at $\alpha = 0$ and $t = \tau$, the approximation

$$r_{\alpha\alpha} \sim (1 - i)\mathrm{sgn}(\alpha)/\tau\,|\alpha|^{½} \tag{8}$$

can be shown to be valid for small values of $|\alpha|$. This means that $C = S \cap \pi$ has a continuously turning tangent at the roll-up point, whereas the curvature of C blows up there.

Recent Progress: A Three-dimensional Analog

It is well known that vortex behavior plays an essential role in generating turbulence in 3D Navier–Stokes equations. The most outstanding open question is whether the 3D Euler equation can develop a finite-time singularity for smooth initial data. One is thus left to wonder whether singularities in 3D vortex sheets are qualitatively different from 2D singularities. Do those singularities, for instance, still appear first in the curvature of S?

It is to questions like these that Thomas Hou, working for the most part with Gang Hu (now at Lehman Brothers) and Pingwen Zhang (of Peking University Beijing), has recently found answers. As described in [3] and presented at the SIAM–EMS conference in Berlin, the researchers have effectively reduced the dimensionality of the Kelvin–Helmholtz singularity problem from three to two.

Hou began his talk in Berlin by exhibiting a three-dimensional analog of (1) for the representation $\mathbf{r}(\alpha_1,\alpha_2,t) = (x(\alpha_1,\alpha_2,t), y(\alpha_1,\alpha_2,t), z(\alpha_1,\alpha_2,t))$ of a vortex sheet S, and considering it in conjunction with an initial condition $\mathbf{r}(\alpha_1,\alpha_2,0) = (\alpha_1,\alpha_2,0) + (\xi_1,\xi_2,\xi_3)$ in which all three of the functions $\xi_i(\alpha_1,\alpha_2,0)$ are presumed to represent small ($= 0(\varepsilon)$) doubly periodic perturbations. He then defined

$$\psi_1 = H_2(\xi_1) - H_1(\xi_2),$$

$$\psi_2 = H_1(\xi_1) + H_2(\xi_2),$$

$$\psi_3 = \xi_3, \tag{9}$$

where H_1 and H_2 are Hilbert transforms [8] in the α_1 and α_2 directions, respectively.

Although this transformation was motivated by properties of the Hilbert (or the Riesz) transform, ψ_1 and ψ_2 have a natural physical interpretation. In some sense, ψ_1 represents a nonlocal projection of all stable modes of the vortex sheet variables, while ψ_2 represents the projection of all unstable modes. As explained below, it is the coupling of the unstable projection ψ_2 with ψ_3 that produces the Kelvin–Helmholtz instability to the leading order. This observation greatly simplifies the analysis of 3D vortex sheet singularities.

Next, he expanded the various transforms $H_i(\partial\xi_j/\partial t)$ in powers of ε, and employed

$$H_1H_2(f) = H_2H_1(f)$$

$$H_1D_2(f) = H_2D_1(f)$$

$$(H_1^2 + H_2^2)(f) = -f$$

$$(H_1D_1 + H_2D_2)(f) = \Lambda(f)\,, \tag{10}$$

in which $D_i = \partial/\partial\alpha_i$ and $\Lambda(f)$ denotes yet another integral transform of f, to conclude that

$$\begin{aligned} \partial\psi_1/\partial t &= O(\varepsilon^2) \\ \partial\psi_2/\partial t &= \frac{1}{2}\gamma D_2^*\psi_3 + O\left(\varepsilon^2\right) \\ \partial\psi_3/\partial t &= -\frac{1}{2}\gamma D_2^*\psi_2 \\ &\quad -\frac{1}{2}\gamma D_1^*\psi_1 + O\left(\varepsilon^2\right). \end{aligned} \tag{11}$$

Here, γ is a constant and $D^*_i = \partial/\partial\beta_i$, while β_1 and β_2 are certain linear combinations of α_1 and α_2. The comparatively simple form of (11) is the result of a number of fortuitous cancellations that occur, thanks to (10), in the course of the derivations. It is clear from (11) that the Kelvin–Helmholtz instability is due to the coupling between ψ_2 and ψ_3 in the β_2 direction.

Because the lines β_1 = constant are vortex lines on S, to which the lines β_2 = constant are orthogonal, the foregoing observations offer new geometric insight into the formation of singularities on 3D vortex sheets. In particular, the fact that the β_1 direction coincides with the direction of the fluid velocity jump from one side of S to the other tends to confirm that the velocity jump is indeed the root cause of the Kelvin–Helmholtz instability. In fact, Hou and co-workers derived a leading-order system that is almost identical to (7). This indicates that the driving mechanism for 3D vortex sheet singularities is essentially two dimensional.

A particularly interesting conclusion concerning the onset of instability emerges from Hou's adaptation of complex singularity tracing methods to three dimensions. When the real variable β_2 is allowed to assume complex values while β_1 remains a fixed real parameter, singularities emerge as curves Γ_t: $(\beta_1, \mathrm{Re}(\beta_2(\beta_1;t)), \mathrm{Im}(\beta_2(\beta_1;t)))$ in a three-dimensional real parameter space. And because (for each fixed t) the second and third coordinates depend analytically on the first, the earliest contact between the curve Γ_t and the plane $\mathrm{Im}(\beta_2) = 0$—and thus the first physical singularity—must occur at an isolated point $(\beta_1, \mathrm{Re}(\beta_2), 0)$ in parameter space corresponding to an equally isolated point P on the vortex sheet S. Otherwise, the real-analytic function $\mathrm{Im}(\beta_2(\beta_1;\tau))$ must vanish identically when $t = \tau$, in which case the entire curve Γ_t drops instantaneously into the plane $\mathrm{Im}(\beta_2) = 0$, and physical singularities must appear simultaneously at every point on a corresponding curve $C_\tau \subset S$. The analyticity of the dependence of β_2 on β_1 prevents first contact between Γ_t and $\mathrm{Im}(\beta_2) = 0$ from occurring along a mere segment of Γ_τ.

The foregoing results were all obtained by formal asymptotic analysis, and therefore require confirmation by high-order, high-resolution numerical analysis. Relevant findings are reported in [4] and [7]. Hou's contribution to the latter activity is a "model equation" in which the integral operator in the 3D analog of the periodic version of (1) is approximated by a convolution operator, which can be evaluated with commendable accuracy by fast Fourier transforms in $O(N^2 \log N)$ flops.

Hou points out that (i) the proposed model equation produces the same tangential velocity jump as the full equation, (ii) the time-series solution at $t = 0$ generates the same 3/2 branch-point singularity as the full equation in the complex α_2-plane, and (iii) the solution S: $\mathbf{r}(\alpha_1,\alpha_2,t)$ of the model equation has, at the physical-singularity time, the same shape as that of the full equation near the singularity point. Moreover, in terms of the β_1 and β_2 variables, the flows seem, as expected, to be "more unstable" in the β_2 direction than in the β_1 direction.

The overall thrust of Hou's work is to show that the driving mechanism for singularity formation in 3D vortex sheets is essentially the same as in 2D vortex sheets. This is rather surprising. Though no one claims to possess a comprehensive understanding of turbulence and hydrodynamic instability, progress toward that ever distant goal continues to be made. Hou and his co-workers seem to have discovered an important new piece of the puzzle.

References

[1] G. Birkhoff, *Helmholtz and Taylor instability*, Proc. Symp. Appl. Math., American Mathematical Society, 13 (1962), 55–76.

[2] S.J. Cowley, G.R. Baker, and S. Tanveer, *On the formation of Moore curvature singularities in vortex sheets*, J. Fluid Mech., 378 (1999), 233–267.

[3] T.Y. Hou, G. Hu, and P. Zhang, *Singularity formation in 3-D vortex sheets*, submitted to *Phys. Fluids*.

[4] R. Krasny, *A study of singularity formation in a vortex sheet by the point vortex method*, J. Fluid Mech., 167 (1986), 65–93.

[5] D.I. Meiron, G.R. Baker, and S.A. Orszag, *Analytic structure of vortex-sheet dynamics, part 1: Kelvin–Helmholtz instability*, J. Fluid Mech., 114 (1982), 283–298.

[6] D.W. Moore, *The spontaneous appearance of a singularity in the shape of an evolving vortex sheet*, Proc. R. Soc. London, A365 (1979), 105–119.

[7] M.J. Shelley, *A study of singularity formation in vortex-sheet motion by a spectrally accurate vortex method*, J. Fluid Mech., 244 (1992), 493–526.

[8] E.M. Stein, *Singular Integrals and Differentiability Properties of Functions*, Princeton University Press, Princeton, New Jersey, 1970.

James Case writes from Baltimore, Maryland.